AMERICAN SOCIETY FOR MICROBIOLOGY | Journal of Virology

Virology | Full-Length Text

HPV-18 E6 enhances the interaction between EMILIN2 and SNX27 to promote WNT signaling

Justyna Broniarczyk,[1,2] Oscar Trejo-Cerro,[1] Paola Massimi,[1] Nežka Kavčič,[1] Michael P. Myers,[1] Lawrence Banks[1]

AUTHOR AFFILIATIONS See affiliation list on p. 15.

ABSTRACT Oncogenic HPV E6 proteins have a PDZ-binding motif (PBM) which plays important roles in both the viral life cycle and tumor development. The PBM confers interaction with a large number of different PDZ domain-containing substrates, one of which is Sorting Nexin 27. This protein is part of the retromer complex and plays an important role in endocytic sorting pathways. It has been shown that at least two SNX27 interacting partners, GLUT1 and TANC2, are aberrantly trafficked due to the E6 PBM-dependent interaction with SNX27. To investigate further which other components of the endocytic trafficking pathway might be affected by the SNX27-HPV E6 interaction, we analyzed the SNX27 proteome interaction profile in a previously described HeLa cell line expressing GFP-SNX27, both in the presence and absence of the HPV-18 E6 oncoprotein. In this study, we identify a novel interacting partner of SNX27, secreted glycoprotein EMILIN2, whose release is blocked by HPV18 E6 in a PBM-dependent manner. Mechanistically, E6 can block EMILIN2 interaction with the WNT1 ligand, thereby enhancing WNT1 signaling and promoting cell proliferation.

IMPORTANCE This study demonstrates that HPV E6 blocks EMILIN2 inhibition of WNT1 signaling, thereby enhancing cell proliferation in HPV-positive tumor cells. This involves a novel mechanism whereby the E6 PBM actually contributes toward enhancing the interaction between SNX27 and EMILIN2, suggesting that the mode of recognition of SNX27 by E6 and EMILIN2 is different. This is the first example of the E6 PBM altering a PDZ domain-containing protein to enhance potential substrate recognition.

KEYWORDS HPV, E6, SNX27, WNT signaling

Human papillomaviruses (HPVs) are small, non-enveloped DNA viruses that infect cutaneous and mucosal epithelial cells and can cause hyperproliferative lesions and cancer development (1). The HPV types that are associated with the development of cervical and other cancers are known as high-risk human papillomaviruses [HR-HPV], and a common characteristic marker of these types is the presence of a PDZ (PSD95/Discs Large/ZO-1)-binding motif (PBM) at the extreme carboxy terminus of the E6 oncoproteins. Through this motif, which is absent in the majority of low-risk HPV types, E6 can interact with a variety of cellular proteins containing PDZ domains, such as Discs Large (DLG1) and Scribble (hScrib), modulating cell polarity and thus regulating the HPV life cycle and HPV-induced malignancies (2–5).

Interestingly, recent studies have identified a novel function of the E6 PBM and linked this to the regulation of endocytic transport pathways. Cancer-causing E6s were found to interact with Sorting Nexin 27 (SNX27), an essential component of the retromer complex, which controls the correct trafficking of a number of PBM-containing endocytic cargoes (6). Unlike most of its PDZ domain-containing targets, E6 does not target SNX27 for degradation. Rather, it has been demonstrated that in HPV-18-positive cell lines, the

Editor Lori Frappier, University of Toronto, Toronto, Canada

Address correspondence to Justyna Broniarczyk, justekbr@amu.edu.pl.

The authors declare no conflict of interest.

See the funding table on p. 16.

Received 24 April 2024
Accepted 20 May 2024
Published 14 June 2024

association of SNX27 with components of the retromer complex and the endocytic transport machinery is altered in an E6 PBM-dependent manner (7).

Analysis of an SNX27 cargo, the glucose transporter GLUT1, reveals E6-dependent maintenance of GLUT1 expression and alteration in its association with components of the endocytic transport machinery. Removal of HR E6 causes a reduction in glucose uptake, while loss of SNX27 results in slower cell proliferation in low nutrient conditions (7). More recently, it was shown that HPV E6 inhibits the association between SNX27 and TANC2, resulting in increased levels of TANC2 and increased rates of cell proliferation, all of which were shown to be dependent upon the E6 PBM (8).

Previous proteomic analyses have indicated a very large SNX27 interactome (9, 10), many of which are believed to be important trafficking cargoes of SNX27. These include transmembrane proteins and soluble accessory proteins (11), and it is likely that E6 may also modulate transport of some of these cargoes. Furthermore, there is emerging evidence to suggest that SNX27 may have a role in the development of human cancer (12, 13). While a precise role of SNX27 in cancer remains unclear, it is noteworthy that many of the previous studies on SNX27 were performed in HeLa cells and, considering the presence of HPV-18 E6 in this cell type, we were interested in determining whether the profile might have been influenced by the HPV-18 E6 oncoprotein. Therefore, to investigate further which other components of the trafficking pathway might be affected by the SNX27-HPV E6 interaction and linked with cancer development, we used a previously-described HeLa cell line expressing GFP-SNX27 (8), and we again analyzed its SNX27 proteome interaction profile in the presence or absence of HPV E6.

In this study, we identify a novel interacting partner of SNX27, secreted glycoprotein EMILIN2, whose interaction with SNX27 is enhanced in an HPV18 E6 PBM-dependent manner, resulting in enhanced WNT1 signalling and enhanced cell proliferation.

RESULTS

Identification of EMILIN2 as a novel-interacting partner of SNX27 in HPV-18-positive HeLa cells

It has been shown before that HPV E6 interacts with SNX27 and can potentially perturb the normal endosomal trafficking of at least two of its interacting cargos, GLUT1 and TANC2 (2, 8). Our earlier proteomic analysis in HPV-18-positive cervical tumor-derived cells demonstrated that E6 can block, in a PBM-dependent manner, the binding of TANC2 to SNX27, thereby promoting increased cell proliferation (8). Therefore, we wanted to analyze further which other PBM cargoes might be affected by endogenous HPV-18 E6. To do this, we used previously described HeLa cell lines, stably expressing GFP-SNX27 (8), transfected with siRNA E6AP to abolish E6 expression (14). Having confirmed 18E6 silencing by western blotting, using increased p53 levels as a surrogate marker (Fig. 1A), we harvested the cells and immunoprecipitated the extracts using anti-GFP antibody-conjugated agarose beads (GFP-trap) to pull down SNX27 and any associated proteins. The samples were then subjected to mass spectrometry analysis. The resulting protein profile obtained from siRNA E6AP-treated cells was compared with that from control siRNA-treated cells, with our focus being on proteins that contain a PBM. One of the most interesting candidates in this analysis was EMILIN2 (Fig. 1B), which has a class I PBM (sequence x-S/T-x-V/I/L-COOH) located at the C-terminus, and which was detected only in the presence of 18E6, suggesting that this is a potential interacting partner of SNX27 whose association might be dependent on the presence of E6. Interestingly, to our knowledge, EMILIN2 has not been identified before in any proteomic approach as an SNX27-interacting partner.

Interactions between EMILIN2 and SNX27 are enhanced by the presence of HPV-18E6 *in vitro* and *in vivo*

Having found by mass spectrometry analysis that EMILIN2 and SNX27 interact in the presence of HPV-18 E6, we next sought to determine whether EMILIN2 and SNX27 can be

A.

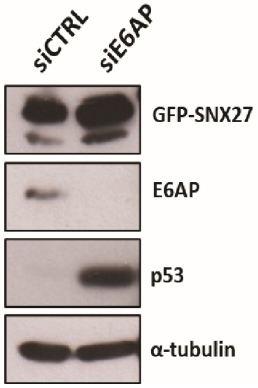

B.

Samples	Protein	Log(e)	Log(l)	%/%	# of peptides	Total
siCTRL	SNX27	-27.7	5.01	7.5/13	4	9½
	EMILIN2	-9.9	4.28	3.4/5	2	2
siE6AP	SNX27	-62.8	5.34	19/24	9	31½
	EMILIN2		-	-	-	-

FIG 1 Identification of EMILIN2 as a novel-interacting partner of SNX27 in HPV-18-positive HeLa cells. (A) Western blot analysis of HeLa cells stably expressing GFP-SNX27, transfected with control siRNA and siRNA targeting E6AP, confirms the silencing of 18E6 protein. (B) Extracts of HeLa cells stably expressing GFP-SNX27 transfected with siRNA control or siE6AP were analyzed by mass spectroscopy. The table shows the identification of EMILIN2 as the prominent SNX27 hit, only in cells transfected with control siRNA. Also shown are E values (the base-10 log of the expectation that the assignment is stochastic), L values (the base −10 log of the sum of the intensities of the fragment ion spectra), protein coverage (% of protein residues /% corrected for unlikely peptides), the number of unique peptide sequences (#), and a total number of tandem mass spectra that can be assigned to each protein.

associated *in vitro* and *in vivo*. To do this, first, we performed a glutathione *S*-transferase (GST) pull-down assay where GST-SNX27 and GST alone were incubated with extracts of HEK293 cells expressing HPV-18 E6, either wild type or the T156E mutant (whose PBM is non-functional). The results in Fig. 2A show that Emilin can interact with SNX27 in the absence of E6; however the presence of HPV-18 E6 enhances EMILIN2 binding to GST-SNX27 in a PBM-dependent manner. In addition, we observed that E6 can bind to GST-SNX27, as expected. To confirm that EMILIN2 and SNX27 also interact *in vivo*, we used a co-immunoprecipitation assay. HEK293 cells were transfected with the EMILIN2-expressing plasmid alone or in combination with a plasmid expressing Flag-tagged SNX27 in the presence and absence of GFP-tagged 18E6. As a control, we used cells transfected only with EMILIN2-expressing plasmid and GFP-tagged 18E6. After 48 h, the cells were harvested, and cell extracts were immunoprecipitated with mouse anti-Flag antibody. Co-immunoprecipitating EMILIN2 was then detected by Western blotting using a mouse anti-EMILIN2 antibody. The results in Fig. 2B demonstrate a clear interaction between EMILIN2 and SNX27 and confirm that SNX27 can bind both EMILIN2 and HPV-18 E6.

The PDZ and the FERM domain of SNX27 are required for EMILIN2 binding

Since both EMILIN2 and HPV-18E6 contain a PBM, we were surprised that HPV-18 could enhance EMILIN2 association with SNX27. To investigate this further, we proceeded to analyze the mechanism of interaction between EMILIN2 and SNX27. First, we performed a pulldown assay using cells expressing EMILIN2 and wild-type SNX27 or mutants of SNX27 lacking the PDZ domain (SNX27ΔPDZ) or the FERM domain (SNX27ΔFERM) (shown schematically in Fig. 3A). As a control, we used cells transfected only with EMILIN2 and pCDNA plasmids. After 48 h, the cells were harvested, and cell extracts were immunoprecipitated with mouse anti-Flag antibody. Co-immunoprecipitating EMILIN2 was then detected by Western blotting using a mouse anti-EMILIN2 antibody. As can be seen from Fig. 3B, the loss of either the PDZ or the FERM domains of SNX27 greatly reduces EMILIN2 association with SNX27, indicating that both the PDZ and the FERM

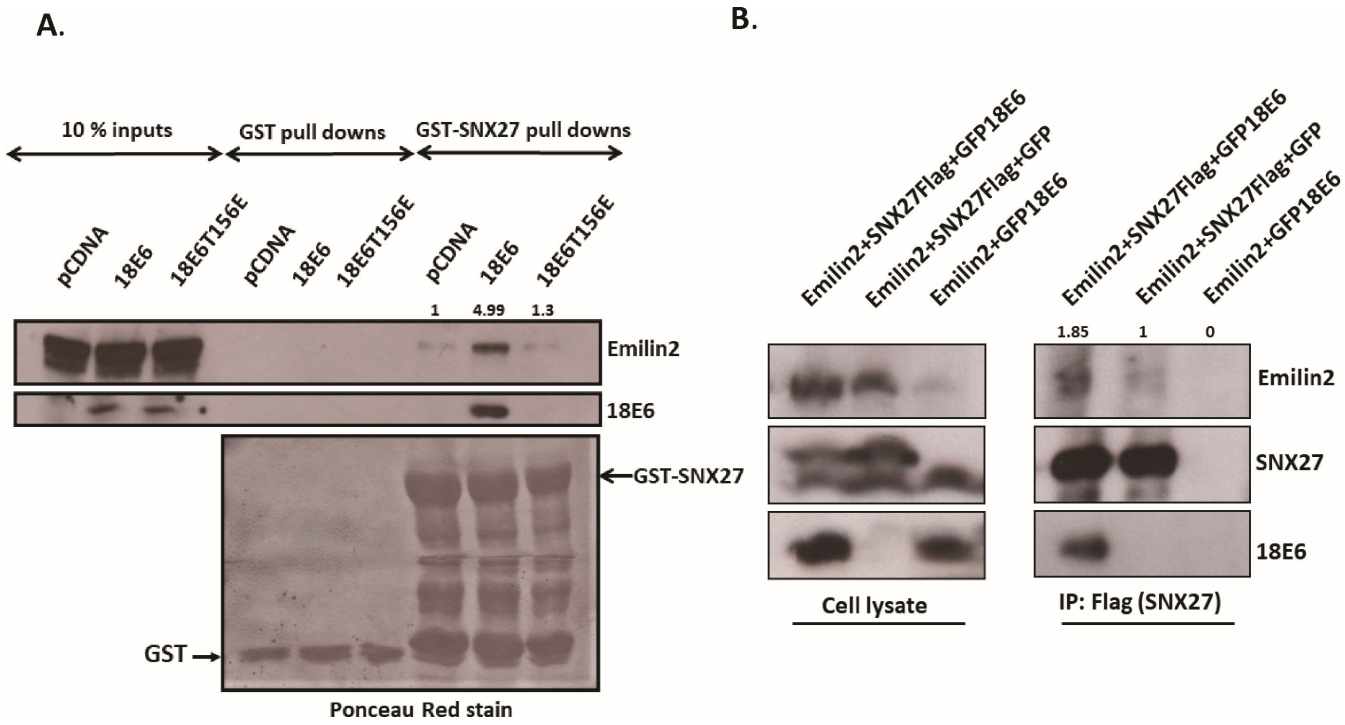

FIG 2 Interactions between EMILIN2 and SNX27 are enhanced in the presence of HPV-18E6 *in vitro* and *in vivo*. (A) HEK293 cells were transfected with plasmids expressing EMILIN2, HA-tagged HPV-18 E6 (HA-18E6) WT, HPV-18 E6 (HA-18E6) ΔPBM mutant, or pCDNA plasmid as a control. After 24 h, the cells were harvested and incubated with GST alone and GST SNX27 fusion proteins. Bound proteins were assessed by Western blotting using an anti-EMILIN2 antibody. For all experiments, the intensity of EMILIN2-SNX27 interactions was assessed by quantifying the pixel intensity of each EMILIN2 band relative to the corresponding intensity of the GST (SNX27) band, using densitometry (ImageJ). The results are shown above the relevant lanes, normalized to the levels of the pCDNA control. Note that more EMILIN2 is pulled down by SNX27 in the presence of E6. (B) EMILIN2 and Flag-SNX27 were expressed in HEK293 cells with or without GFP18E6. Extracts were immunoprecipitated with an anti-Flag antibody, and coimmunoprecipitated EMILIN2 was detected on immunoblot with an anti-EMILIN2 antibody, confirming the EMILIN2/SNX27/18E6 complex. The intensity of EMILIN2-SNX27 interactions was assessed by quantifying the pixel intensity of each EMILIN2 band relative to the corresponding intensity of the SNX27 band, using densitometry (ImageJ). The results are shown normalized to levels of the interactions of EMILIN and SNX27 in the absence of 18E6.

domains of SNX27 are required for EMILIN2 binding. Next, to determine whether HPV-18E6 can affect the interaction between EMILIN2 and SNX27 mutants, we repeated the experiment, transfecting HEK293 cells with EMILIN2 and wild-type SNX27 or SNX27ΔPDZ or SNX27ΔFERM, in the presence of HPV-18E6. As expected, and can be seen in Fig. 3C, the loss of either the PDZ or the FERM domain of SNX27 greatly reduces EMILIN2 association with SNX27, confirming that both the PDZ and the FERM domains of SNX27 are required for EMILIN2 binding. HPV-18E6 binding to SNX27 was found to be dependent on the PDZ domain present on SNX27, as expected. Interestingly, we also observed that the FERM domain seems to be required for an efficient E6-SNX27 interaction.

HPV-18E6 blocks the release of EMILIN2 into the medium in a PBM-dependent manner

Having shown that HPV-18 E6 can enhance the association between EMILIN2 and SNX27, we wanted to determine how this might be reflected in changes to the levels of EMILIN2 protein. As EMILIN2 is a secreted glycoprotein, we decided to determine whether HPV-18E6 and SNX27 can affect the levels of intracellular and secreted EMILIN2.

To do this, HEK293 cells were transfected with EMILIN2-expressing plasmid, alone or in combination with HA-tagged HPV-18 E6, either wild-type or the T156E mutant (whose PBM is non-functional). After 24 h, the medium was replaced with serum-free medium for 24 h. Cell lysates and concentrated cell medium were analyzed by western blot, using

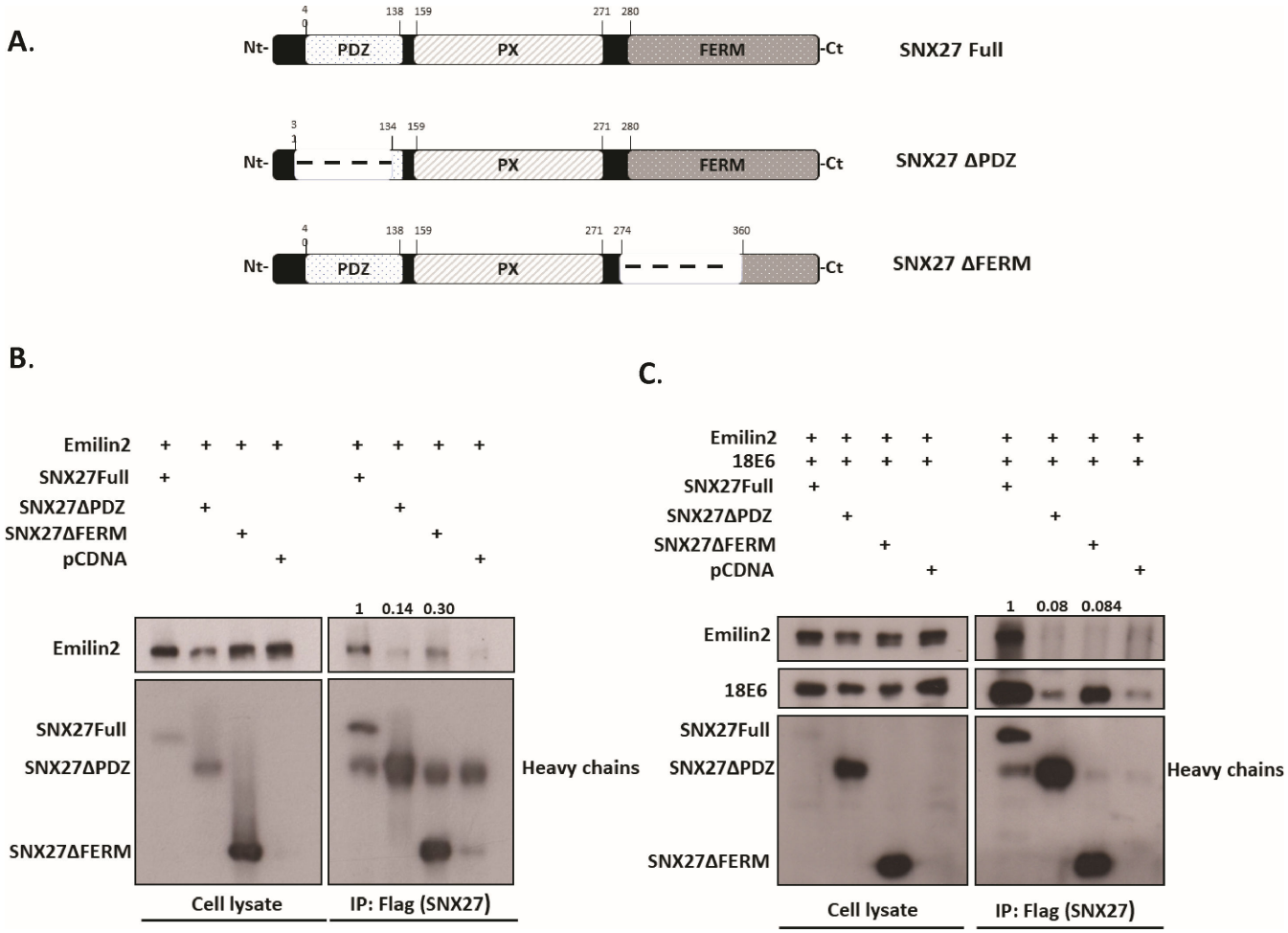

FIG 3 The PDZ and the FERM domain of SNX27 are required for EMILIN2 binding. (A) Schematic of full-length SNX27 and the SNX27ΔPDZ and ΔFERM mutants. (B) HEK293 cells were transfected with plasmids expressing EMILIN2, full-length Flag-tagged SNX27, and deletion mutants of SNX27 or pCDNA plasmid as a control. Extracts were immunoprecipitated with an anti-Flag antibody, and coimmunoprecipitated EMILIN2 was detected on immunoblot with an anti-EMILIN2 antibody, while SNX27 was detected using a mouse anti-FLAG antibody. For all experiments, the intensity of EMILIN2-SNX27 interactions was assessed by using densitometry (ImageJ) to quantify the pixel intensity of each immunoprecipitated EMILIN2 band, relative to the corresponding intensity of the immunoprecipitated SNX27 band. The results are shown normalized to levels of the interactions of EMILIN and SNX27 wild type. (C) HEK293 cells were transfected with plasmids expressing EMILIN2, full-length Flag-tagged SNX27, deletion mutants of SNX27, or pCDNA plasmid as a control, in the presence of 18E6. Extracts were immunoprecipitated with an anti-Flag antibody, and coimmunoprecipitated EMILIN2 and 18E6 were detected on immunoblot with anti-EMILIN2 and anti-18E6 antibodies, while SNX27 was detected using a mouse anti-FLAG antibody. For all experiments, the intensity of EMILIN2-SNX27 interactions was assessed by quantifying the pixel intensity of each immunoprecipitated EMILIN2 band, relative to the corresponding intensity of the immunoprecipitated SNX27 band using densitometry (ImageJ). The results are shown normalized to levels of the interactions of EMILIN and SNX27 wild type in the presence of 18E6 protein.

α-HA to detect E6, α-EMILIN2, and α-β-galactosidase antibodies. As can be seen from Fig. 4A, the presence of HPV-18 E6 has no major effect on total EMILIN2 levels in HEK293 cells, but blocks the release of EMILIN2 into the medium in a PBM-dependent manner.

To determine whether SNX27 can also affect EMILIN2 levels inside and outside cells, we repeated the experiment transfecting HEK293 cells with EMILIN2-expressing plasmid, alone or with plasmids expressing either HA-tagged HPV-18 E6, Flag-tagged SNX27, or both together. As can be seen in Fig. 4B, the presence of HPV-18 E6 and SNX27 does not affect intracellular levels of EMILIN2. As would be expected, the presence of HPV-18 E6 blocks the release of EMILIN2 into the medium, but surprisingly SNX27 alone has no effect on EMILIN2 secretion. Interestingly, the presence of both HPV-18 E6 and SNX27 significantly increased the secretion of EMILIN2, suggesting that overexpression of SNX27 can counteract the E6 effects.

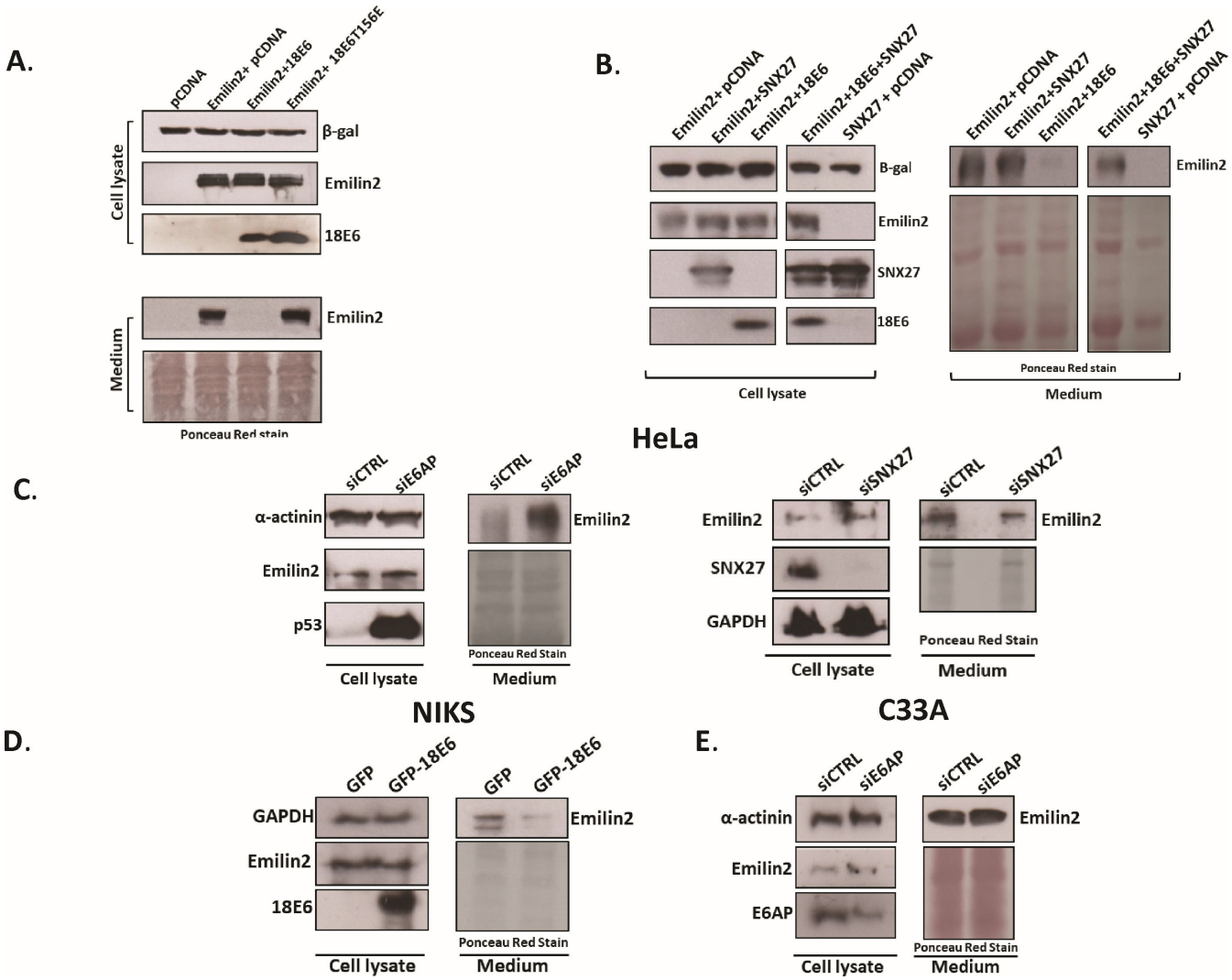

FIG 4 HPV-18E6 blocks the release of EMILIN2 into the medium in a PBM-dependent manner. (A) EMILIN2, alone or with HA-18E6 or HA-18E6T156E (ΔPBM mutant), was expressed in HEK293 cells. After 24 h, the medium was replaced with a serum-free medium for 24 h. Cell lysates and concentrated cell medium were analyzed by western blot, using α-HA to detect E6, α-EMILIN2, and α-β-galactosidase antibodies. (B) EMILIN2 was expressed in HEK293 cells alone, with SNX27, with 18E6, or with 18E6 plus SNX27. After 24 h, the medium was replaced with serum-free medium for 24 h. Cell lysates and concentrated medium were analyzed by western blot, as before. (C) HeLa cells were transfected with scrambled siRNA as a control and siRNA E6AP to silence 18E6 (left panel) or with scrambled siRNA as a control and siRNA SNX27 to silence SNX27 protein. After 48 h, the medium was replaced with a serum-free medium for 24 h. Equal amounts of concentrated proteins were immunoprecipitated using an anti-EMILIN2 antibody. Cell lysates and immunoprecipitated EMILIN2 in concentrated cell medium were analyzed by western blot, using anti-EMILIN2, anti-p53 antibody to confirm E6 silencing, anti-SNX27 antibody to confirm SNX27 silencing, anti-α-actinin and anti-GAPDH antibodies to monitor protein loading. (D) NIKS, expressing either wild-type HPV-18 E6 or empty GFP as a control were grown in serum-free medium for 24 h. Cell lysates and concentrated medium were analyszed by western blot, using anti-EMILIN2, anti-18E6 antibody and anti-GAPDH antibody to monitor protein loading. (E) C33A cells were transfected with scrambled siRNA as a control and siRNA E6AP. After 48 h, the medium was replaced with a serum-free medium for 24 h. Cell lysates and concentrated cell medium were analyzed by western blot, using anti-EMILIN2, anti-E6AP antibody, and anti-α-actinin antibody to monitor protein loading.

To confirm further that EMILIN2 secretion can be affected by E6 and SNX27, we repeated the experiment using HPV-18-positive HeLa cells. First, this cell line was transfected with either scrambled siRNA as a control or siRNA E6AP to knock down the HPV E6 protein (14). Cell lysates and secreted EMILIN2 were analyzed by western blot. As can be observed in Fig. 4C (left panel), loss of E6 has no major effect on total EMILIN2 levels in HeLa cells but significantly increases the release of EMILIN2. Interestingly, when we repeated the experiment using HPV-18-positive HeLa cells transfected with

scrambled siRNA as a control or siRNASNX27 to knock down the SNX27 protein, as expected, we observed that loss of SNX27 has no major effect on total EMILIN2 levels in HeLa cells but seems to decrease the release of EMILIN2 (Fig. 4C, right panel).

To further validate the effect of HPV18 E6 protein on EMILIN2 release in a more physiologically relevant setting, we repeated the experiments using Normal Immortalised Keratinocytes (NIKS), stably expressing either wild type HPV-18 GFP-E6 or empty GFP as a control. Cell lysates and secreted EMILIN2 were analyzed by western blot. As expected and can be seen in Fig. 4D, the presence of E6 has no major effect on total EMILIN2 levels in NIKS cells but significantly blocks the release of EMILIN2. To provide additional evidence that EMILIN2 release is regulated by HPV 18E6 protein, we performed similar experiments using HPV-negative C33A cells, transfected with scrambled siRNA as a control and siRNA E6AP. The Western blotting results in Fig. 4E show that loss of E6AP does not affect EMILIN2 level and release in HPV-negative cell lines, confirming that EMILIN2 release is regulated by HPV 18E6 protein.

EMILIN2 affects HPV-18E6 localization in a PBM-dependent manner

To determine the mechanism by which HPV-18E6 reduces EMILIN2 secretion, we performed an immunofluorescence analysis. To do this, HEK293 cells were transfected with GFP-tagged HPV-18 E6 WT or HPV-18 E6ΔPBM, in the presence or absence of an EMILIN-expressing plasmid. As can be seen from Fig. 5, EMILIN 2 is expressed in a punctate manner typical of the normal pattern of EMILIN2 expression (15) and its distribution is not affected by the presence of HPV-18 E6 WT or HPV-18 E6ΔPBM. Interestingly in cells co-transfected with EMILIN-expressing plasmid, HPV-18E6 is seen in both nucleus and cytoplasm; while in cells co-transfected with empty pCDNA plasmid, HPV-18E6 is located mainly in the nucleus, as previously reported (16). However, the localization of HPV-18 E6ΔPBM did not change in the presence of overexpressed EMILIN2, suggesting that EMILIN2 affects HPV-18E6 localization in a PBM-dependent manner.

EMILIN2 reduces cell proliferation through a WNT-induced signaling pathway and interaction with the WNT1 ligand in the absence of the E6 PBM domain

As has already been shown, both EMILIN2 and HPV-18 E6 oncoprotein can independently affect tumor cell viability and proliferation through regulation of the WNT/β-catenin signaling pathways, we, therefore, sought to determine whether a similar mechanism was operative here (17, 18). As it had previously been shown that EMILIN2 decreases tumor cell viability (17, 19), we first decided to investigate whether overexpression of EMILIN2 can affect the proliferation of cells ectopically expressing HPV-18 E6 WT or HPV-18 E6ΔPBM mutant. To do this, we performed a colony-forming assay in HaCaT cells transfected with plasmids expressing HPV-18E6 WT or HPV-18 E6ΔPBM mutant, in the absence or presence of EMILIN2. The cells were then subjected to G418 selection, after which the colonies were stained with Giemsa and counted. The results shown in Fig. 6 indicate that overexpression of HPV-18E6, in the presence or absence of EMILIN2, slightly changes the formation of colonies. Interestingly, we observed a dramatic difference in the number of colonies when the HPV-18 E6ΔPBM mutant was overexpressed in the presence of EMILIN2, suggesting that EMILIN2 can reduce the proliferation of cells in the absence of a functional E6 PBM.

Next, we queried whether the WNT signaling pathway can regulate this process. HEK293 cells were transiently transfected with a TCF-4-dependent luciferase reporter plasmid (TOPFLASH) and a β-catenin-expressing plasmid in the presence or absence of plasmids expressing EMILIN2 and HPV-18E6 WT or HPV-18 E6ΔPBM, as indicated. After 48 h, immunoblot assays were performed, confirming the expression of β-catenin, EMILIN2, and GFP-tagged E6 proteins (Fig. 7A left panel).

As can be seen in the right panel of Fig. 7, TCF-4 transcriptional activity was significantly decreased (by around 50%) upon ectopic expression of EMILIN2 in the presence of β-catenin, compared with cells without EMILIN2 overexpression. Interestingly, TCF-4

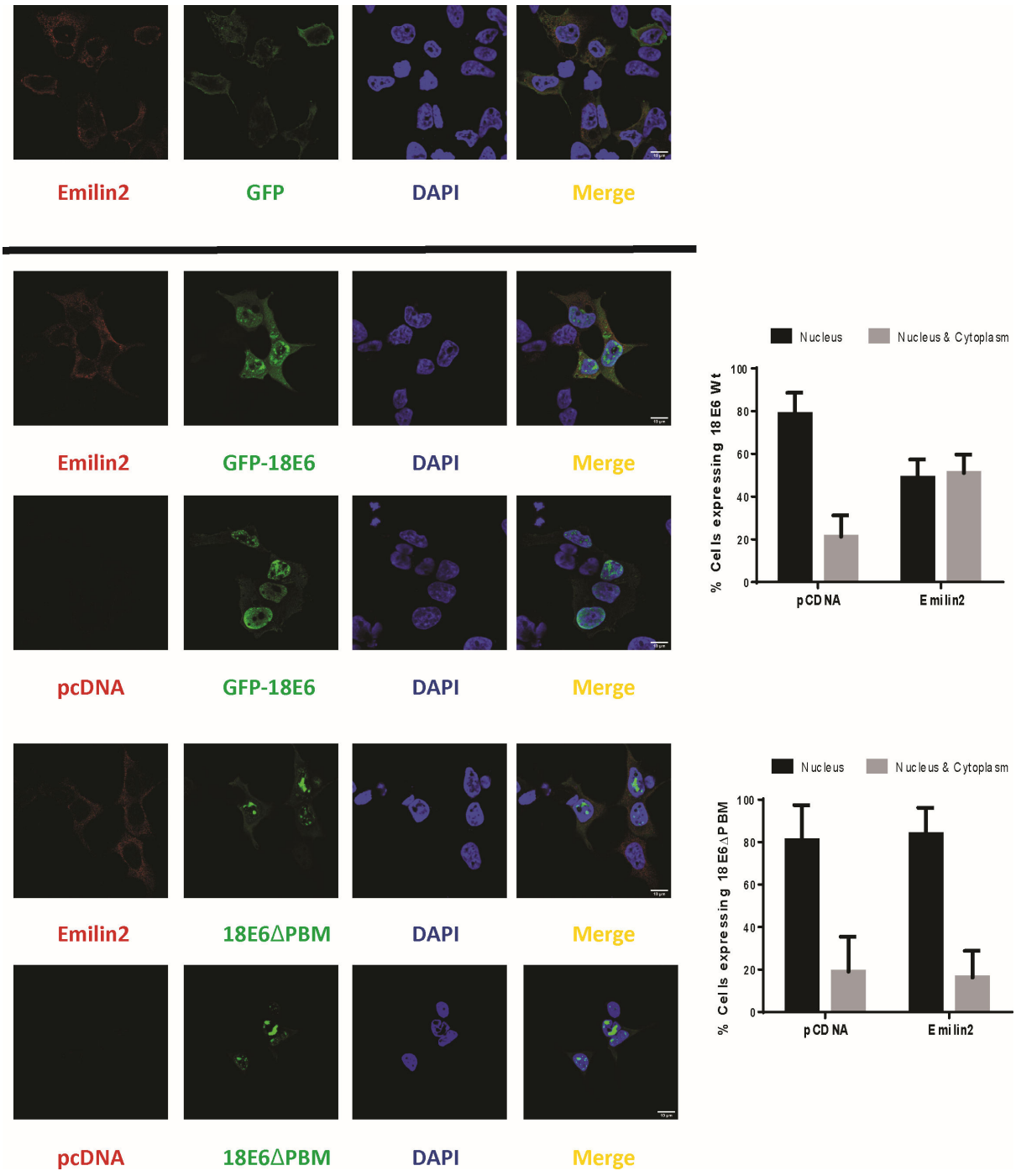

FIG 5 EMILIN2 effects on HPV-18E6 localization are PBM-dependent. GFP-18E6 or −18E6ΔPBM were expressed, with or without EMILIN2, in HEK293 cells. Immunofluorescent analyses with anti-EMILIN2 (red) and anti-GFP (green) antibodies show that EMILIN2 alters the localization of GFP-18E6 but not GFP-18E6ΔPBM. Representative images are shown (left panel). Quantification of GFP-18E6 and GFP-18E6ΔPBM distribution within the nucleus or nucleus and cytoplasm compartments is also shown (right panel) based on the percentage of cells expressing GFP-18E6 and GFP-18E6ΔPBM.

transcriptional activity was not substantially affected by EMILIN2 in the presence of HPV-18 E6 WT, but it was similarly reduced (around 50%) by EMILIN2 in the presence of HPV-18 E6ΔPBM.

It is well-known that EMILIN2 binds to the WNT1 ligand (17). Therefore, to confirm further that EMILIN2 inhibits WNT1-induced signaling in the absence of a functional E6 PBM domain, we examined whether the presence of HPV-18 E6 WT or HPV-18 E6ΔPBM

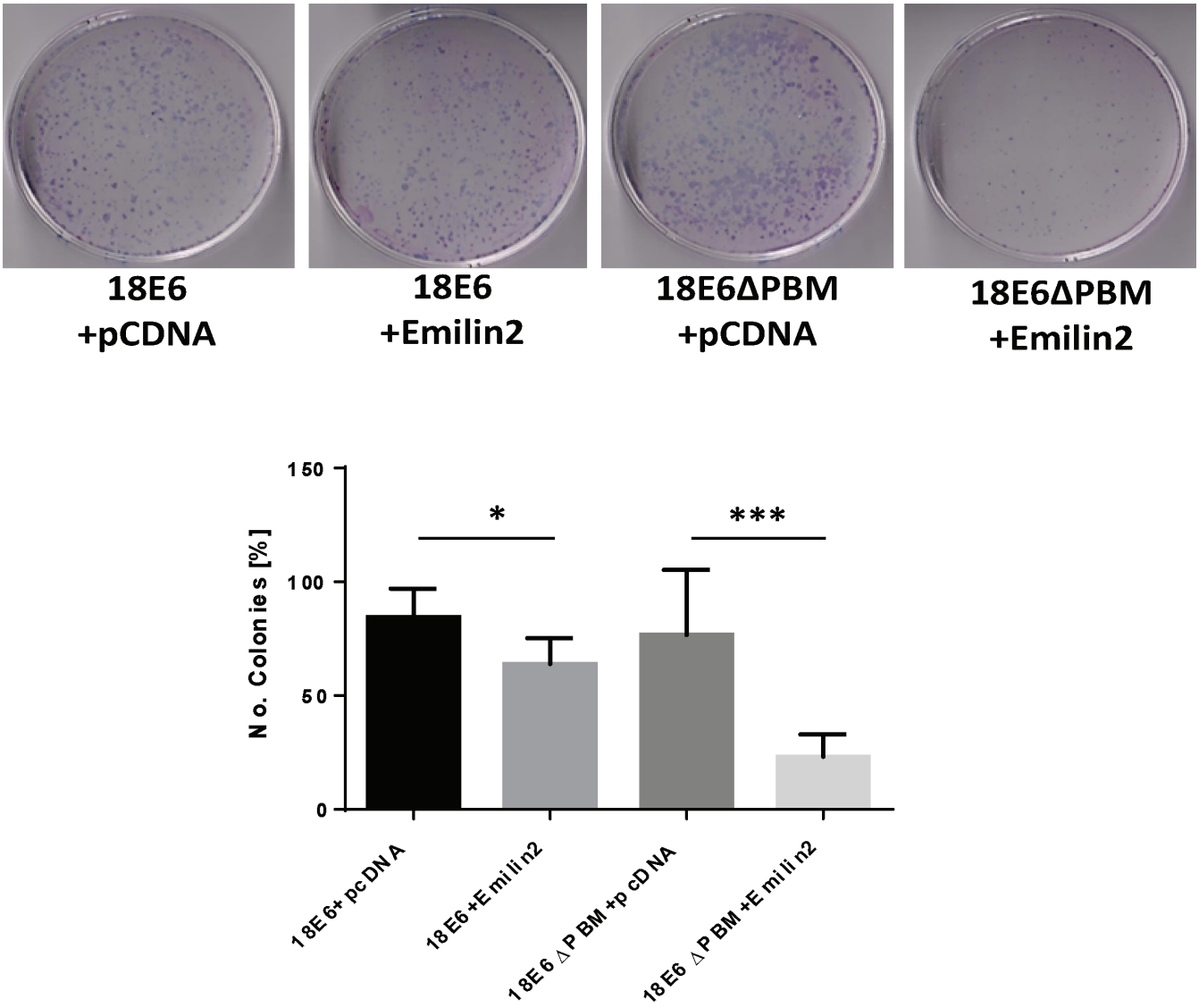

FIG 6 EMILIN2 reduces cell proliferation in the absence of a functional E6 PBM. HaCaT cells expressing HPV-18E6 or −18E6ΔPBM EMILIN2, were G418-selected for 2–3 weeks. Colonies were counted with countPHICS software. Top representative images; bottom quantification histogram shows means from 3 independent assays and standard deviations (*$P < 0.1$; ***$P < 0.001$).

mutant could affect those interactions. HEK293 cells were transfected with plasmids expressing EMILIN2, Flag-tagged SNX27, and V5-tagged WNT1 in the presence of GFP-tagged 18E6 wild type or 18E6ΔPBM mutant. As a control, we used cells transfected with all constructs except the V5-tagged WNT1 plasmid. After 48 h, the cells were harvested, and cell extracts were immunoprecipitated with mouse anti-V5 antibody. Co-immunoprecipitating EMILIN2 and SNX27 were then detected by Western blotting using a mouse anti-EMILIN2 antibody and a mouse anti-Flag antibody, respectively. As would be expected, and can be seen in Fig. 7B, the presence of HPV-18 E6 inhibits the binding of EMILIN2 to the WNT1 ligand in a PBM-dependent manner. Interestingly, HPV-18 E6 has a similar inhibitory effect on the interaction of SNX27 with WNT1.

All these data suggest that HPV-18 E6 blocks EMILIN2 release in a PBM-dependent manner, possibly to prevent EMILIN2 binding to the WNT1 ligand, thereby blocking WNT signaling, which could lead to reduced cell proliferation.

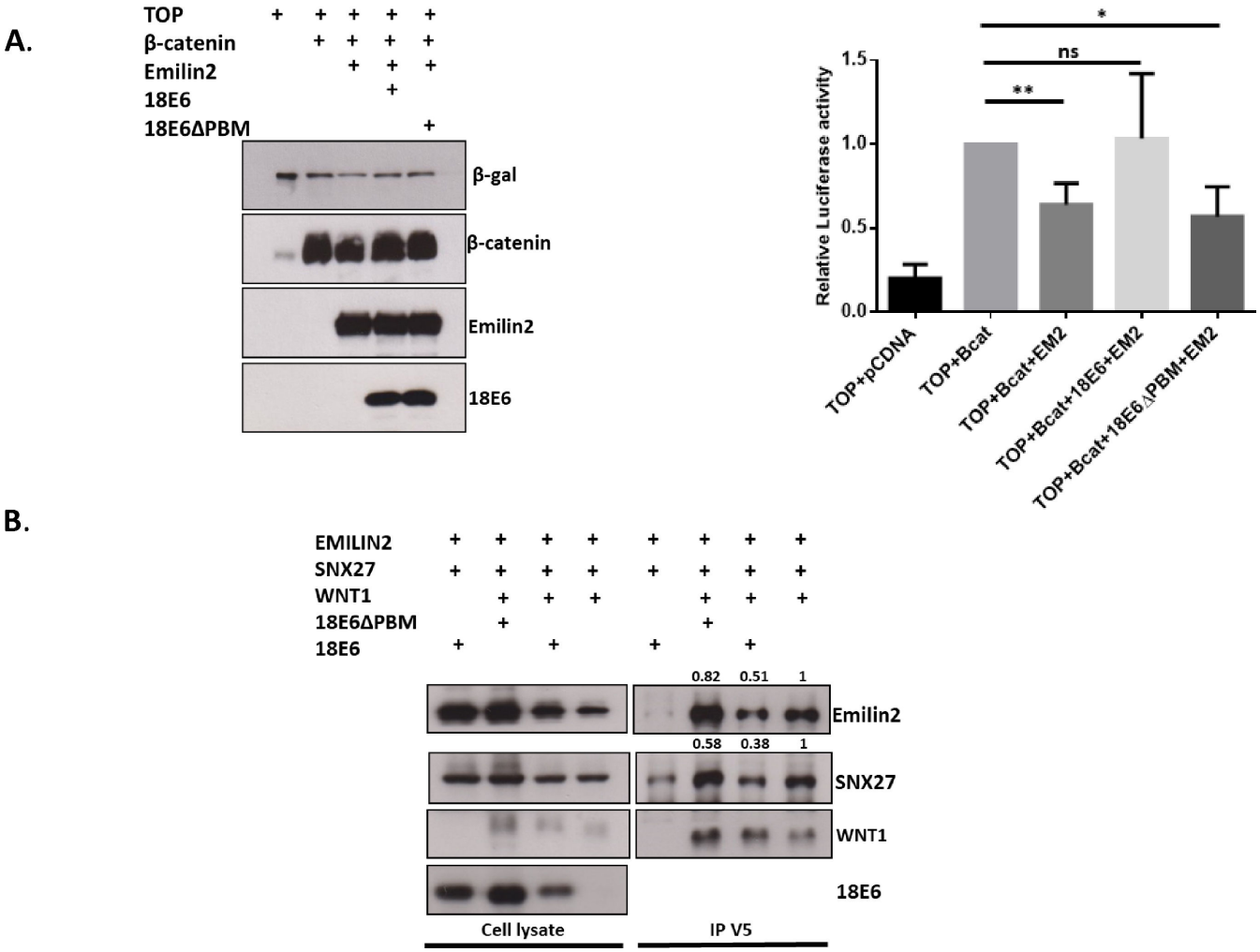

FIG 7 EMILIN2 inhibits WNT1-induced signaling through binding to WNT1 in the absence of a functional E6 PBM. (A) HEK293 cells expressing EMILIN2 ± HPV-18E6 or HPV-18E6ΔPBM and β-catenin were transfected with TOPflash reporter plasmid (TOP) and β-galactosidase reporter plasmids. Immunoblot confirms protein expression (left panel). β-catenin activity was detected by measuring the luciferase activity, normalized for Renilla. Histogram compares luciferase activities with β-catenin levels from three independent assays with standard deviations (*P < 0.1; **P < 0.01; ns, nonsignificant), (right panel). (B) EMILIN2, Flag-SNX27, V5-WNT1, plus or minus GFP18E6, or HPV-18E6ΔPBM were expressed in HEK293 cells. Extracts were immunoprecipitated with an anti-V5 antibody, and coimmunoprecipitated EMILIN2 was detected on immunoblot with an anti-EMILIN2 antibody, while SNX27 was detected using a mouse anti-FLAG antibody. For all experiments, the intensity of EMILIN2-WNT interactions was assessed by quantifying the pixel intensity of each EMILIN2 band relative to the corresponding intensity of the WNT band, while the intensity of SNX27-WNT interactions was assessed by quantifying the pixel intensity of each SNX27 band relative to the corresponding intensity of the immunoprecipitated WNT band using densitometry (ImageJ). The results are shown normalized to levels of pcDNA control. Note that the presence of HPV-18E6 reduces the interactions of EMILIN2 and SNX27 with WNT1 in a PBM-dependent manner.

DISCUSSION

The major role played by the two viral oncoproteins, E6 and E7, in HPV-induced malignancy is well-known; however, not all functions of these proteins are entirely understood.

A unique feature of oncogenic HPV E6 protein is the presence of a Class I PDZ-binding motif (PBM) at its carboxy terminus, which is absent in E6 from benign HPV types, indicating that the PBM is a signature for oncogenic potential (2, 4). Increasing evidence suggests that the HPV E6 PBM domain may mediate cancer development and/or progression by regulating endocytic transport pathways. Early proteomic analyses have shown that the HPV18 E6 PBM interacts with the components of the endocytic sorting machinery, such as Sorting Nexin 27 (SNX27), an essential element of the retromer

complex (6). It has been shown that at least two SNX27 interacting partners, GLUT1 and TANC2, are aberrantly trafficked as a result of the E6 PBM-dependent interaction with SNX27 and thereby contribute to the development of HPV-induced malignancies (8).

In this report, we present new insights into the effect of the HPV E6 PBM domain on an SNX27-binding partner. To explore further which SNX27 cargoes can be altered by HPV E6, we decided to repeat the previously described analysis of the SNX27 proteome interaction profile in the presence or absence of HPV E6.

Mass spectrometry identified a number of SNX27-interacting proteins, of which the most interesting was EMILIN2 (Elastin microfibril interface-located protein 2), as it had not previously been described as an SNX27 binding partner. EMILIN2 was detected only in the presence of HPV E6 and contains a class I PBM (LSHL) located at the C-terminus.

EMILIN2 is a secreted glycoprotein that belongs to the EDEN protein family (20, 21), which plays various roles in the extracellular matrix (ECM), particularly in tissues requiring elasticity and resilience. EMILIN2 contributes to the structural integrity of tissues by interacting with other ECM proteins, such as elastin and fibrillin. It helps in organizing and stabilizing the extracellular matrix, especially in tissues like blood vessels and skin. Dysregulation of EMILIN2 expression or function is associated with various pathological conditions, including cardiovascular diseases, cancer, and connective tissue disorders (20, 21).

ECM is an essential component of the tumor microenvironment, which plays a crucial role in cancer progression and development, regulating cell proliferation, adhesion, invasion, and migration (22). Therefore, as an ECM molecule, EMILIN-2 exerts an important function in a number of tumor types, such as breast, gastric, colorectal, kidney, and ovarian cancers (17, 23–26).

Sorting Nexin 27 contains an N-terminal PDZ domain (Post-Synaptic Density-95/Discs-Large/Zonula Occludens), central PX domain, and C-terminal FERM domain (4.1/Ezrin/Radixin/Moesin). The SNX27 PDZ domain binds PBM cargoes such as transmembrane and cytosolic proteins, which contain type I PDZ-binding motifs (PBM) (11, 27–31). The FERM domain regulates the interactions with endosomal cargoes and can also serve as a signaling complex scaffold (32, 33). It has been shown that the FERM domain binds Ras GTPases (32) and recycling cargoes carrying NPxY/NxxY motif (33).

Here, we show that EMILIN2 binding requires the PDZ and the FERM domains of SNX27 and both PBM and NxxY motifs are present in the EMILIN2 protein sequence. Therefore, it was tempting to speculate that E6's association with SNX27 through its PBM might somehow enhance EMILIN2's association with the SNX27 FERM domain, thereby preventing EMILIN2 secretion. However, when we repeated the assay in the presence of 18E6, we found that 18E6 also requires both PBM and NxxY motifs to bind SNX27, which is in agreement with previous data (7). More studies are needed to explain the mechanism of the EMILIN2, SNX27 and E6 association.

Recent studies showed that the interaction of SNX27 with another extracellular matrix component—degrading enzyme MT1-MMP—is critical for recycling MT1-MMP to the cell surface, which promotes breast cancer metastasis (34). It is also interesting to note that, unlike the other known SNX27 binding partners, MT1-MMP lacks a PBM. Instead, the cytosolic tail of MT1-MMP harbors a DKV motif that closely resembles a Class-III PDZ-binding motif sequence of X[DE]Xφ, where X represents any amino acid and φ represents a hydrophobic residue (35). All this confirms that SNX27 can interact with different ligands through diverse domains and motif associations.

EMILIN-2 expression is often down-regulated during tumor progression; however, the impact of this loss has not been explored, thus far. It has been reported that EMILIN2 affects the activation of the Wnt/β-catenin signaling pathway, a key regulator in the development of many cancers, thus down-modulating cell proliferation and migration (17). It has also been shown that EMILIN-2 influences angiogenesis by triggering IL-8 expression via the EGFR/EGF pathway, thus affecting vessel development and perfusion (36).

In this study, we confirm that, in a PBM-dependent manner, HPV-18 E6 enhances the interaction between EMILIN2 and SNX27, consequently blocking the release of EMILIN2. To examine potential mechanisms for the reduced secretion of EMILIN2 in the presence of E6, we performed an immunofluorescence analysis which showed that EMILIN2 affects HPV-18E6 localization in a PBM-dependent manner. Ectopic co-expression of EMILIN2 with E6 WT dramatically increases the pool of cytoplasmic E6, whereas the nuclear localization of the E6 PBM mutant does not change. All this suggests that the E6 PBM domain might play an essential role in blocking EMILIN2 release from cells, inducing translocation of E6, in the presence of EMILIN2, to the cytoplasm.

Previous studies have shown that EMILIN2 down-modulates the WNT signaling pathway and suppresses breast cancer cell growth and migration (17). As HPV E6 and SNX27 have also been shown to regulate the WNT signaling pathway independently (18, 37, 38), we decided to determine whether this could also be the case here.

First, in a colony formation assay, there was little difference in the numbers of colonies obtained upon overexpression of either EMILIN2, or HPV-18 E6 WT, or both together; however, there was a dramatic reduction in the number of colonies obtained when the HPV-18 E6ΔPBM mutant and EMILIN2 were expressed together. This suggests that EMILIN2 can reduce cell proliferation in the absence of functional E6 PBM and, again, confirms the importance of this domain. The next question raised by this observation was: could the observed difference in cell growth be regulated by the WNT signaling pathway, similarly to breast cancer cells? The analysis confirmed our hypothesis, showing that EMILIN2 alone, and in the presence of HPV-18 E6ΔPBM, significantly reduced the activation of the WNT signalling pathway. Interestingly, this effect was not observed when EMILIN2 and E6 WT were ectopically expressed together, confirming the critical role of the PBM domain.

A fundamentally essential role in the transduction of the WNT signalling pathways is played by secreted glycoproteins such as WNT1, which can activate intracellular signaling pathways by binding to different receptors, such as Frizzled receptors. Interestingly, previous studies showed that as a result of sequence homology with the cysteine-rich domain (CRD) of the Frizzled receptors, EMILIN2 could affect WNT signaling activation through interaction with the WNT ligand (17). To determine whether the same mechanism might be operative in this case, we decided to check whether the presence of HPV-18 E6 could affect the interactions of EMILIN2 with the WNT1 ligand. Our results confirmed that the presence of HPV-18 E6 inhibits the binding of EMILIN2 to the WNT1 ligand in a PBM-dependent manner. Interestingly, HPV-18 E6 has the same inhibitory effect on the interaction of SNX27 with WNT1.

All these data suggest that HPV-18 E6 blocks EMILIN2 release in a PBM-dependent manner. In addition, E6 prevents the interaction of EMILIN2 with WNT1 ligand and the consequent inhibition of WNT signalling, which could lead to reduced cell proliferation.

In this study, we have shown a novel mechanism by which HPV E6 may regulate the WNT signaling pathway. Previous data had reported that both E6 and SNX27 control the WNT signaling pathway independently, using different mechanisms. It has previously been reported that ectopically expressed E6 significantly augments the Wnt/beta-catenin signaling response in a dose-dependent manner, and that this activity is independent of the ability of E6 to target p53 for degradation or to bind PDZ-containing targets (39). However, recent data show that HPV18 E6 promotes cervical cancer cell migration and invasion by reducing the levels of its PDZ-containing target, MAGI3, which leads to the activation of Wnt/β - catenin signalling (40). Other reports show that E6 proteins can up-regulate TCF-4 transcriptional activity to promote overexpression of Wnt target genes, and that E6 and E6*I bind to TCF-4 and β-catenin, impacting TCF-4 stabilization (41).

While several studies implicate HPV E6 in the activation of the canonical Wnt/β-catenin pathway, SNX27 was shown to inhibit the activation of the Wnt signaling pathway. SNX27 interacts with Frizzled (Fzd) receptors to regulate the endocytosis and stability of Fzd, inhibiting canonical Wnt signaling (37). Another report shows the

importance of the C-terminal PBM of SNX27 for the transcriptional activity of β-catenin and proposes that SNX27 might be involved in the endosomal assembly of β-catenin complexes and induce a decrease in the transcriptional activity of β-catenin (38).

As HPV E6 induces activation of WNT signaling to promote cancer cell migration and invasion while EMILIN2 and SNX27 downregulate this pathway, it is possible that E6 enhances the intracellular interaction of EMILIN2 and SNX27 to prevent EMILIN2 secretion. This is also supported by the increased cytoplasmic pool of E6 in the presence of EMILIN2, and the increased interaction of SNX27 with WNT1 in the absence of HPV E6. Interestingly, our data confirm the essential role of the E6 PBM in this process. We proved that the E6 PBM has a crucial effect on the interaction of EMILIN2 with SNX27 and on EMILIN2's secretion and binding to the WNT1 ligand, which, as a consequence, activates the WNT signaling pathway and reduces cell proliferation. Interestingly, previous reports have shown that HPV oncoproteins can modulate extracellular matrix components, such as matrix metalloproteinases. HPV E6 has been also shown to interact with Laminin-5, an ECM protein involved in cell adhesion and migration. Additionally, HPV E6 can activate various signaling pathways involved in ECM remodeling, such as the PI3K/Akt pathway (42, 43). However, further studies are needed to understand this mechanism better, especially in E6-induced malignancy. This work shows that SNX27 can interact with different ligands through diverse PDZ or FERM domain associations and that the E6 PBM domain can modulate SNX27 cargo binding, trafficking, and mode of action and identifies a novel function of the E6 PBM domain in cancer development.

MATERIALS AND METHODS

Cells and transfection

HaCaT, HEK293, and HeLa wild type (ATCC) and GFP-SNX27 HeLa cells were maintained in Dulbecco's modified Eagle's medium (DMEM), supplemented with 10% Fetal Calf Serum (Life Technology), penicillin-streptomycin (100 U/mL), and glutamine (300 µg/mL). Cells were cultured at 37°C with 10% CO2. HeLa cell lines stably expressing GFP-SNX27 were generated as described previously (8). To generate the NIKS (Normal Immortalised Keratinocytes) (44) stably expressing GFP-18E6 and GFP, NIKS were transfected with GFP-18E6 and GFP empty plasmids as control and subjected to hygromycin selection for over 2 weeks. After this time, single-cell clones were picked and then analyzed by Western blotting for GFP-18E6 and GFP, using mouse anti-GFP antibody (Santa Cruz). Cells were maintained in F medium (0.66 mM Ca^{2+}) composed of three parts Ham's F12 medium to one part Dulbecco's modified Eagle's medium and supplemented with the following components: 5% fetal bovine serum (FBS), adenine (24 µg/mL), cholera toxin (8.4 ng/mL), epidermal growth factor (10 ng/mL), hydrocortisone (2.4 µg/mL), and insulin (5 µg/mL).

HeLa cells were transfected with siRNA using Lipofectamine RNAiMAX transfection reagent (Invitrogen). The E6AP siRNA Smart Pool (Dharmacon) was used, while the scrambled siSTABLE nontargeting siRNA was used as a control. For HEK293 cell transfections, calcium phosphate precipitation was used, as described previously (45).

Plasmids

pGWI HA-18E6WT, pGWI HA-18E6T156E, which is defective for PDZ domain binding, pHAHA-GFP18E6 and pHAHA-GFP18E6ΔPBM have been described previously (46, 47). The pcDNA3.1-EMILIN2 construct was kindly provided by Maurizio Mongiat and has been described previously (19). Constructs expressing GST-tagged SNX27, GST-tagged SNX27 PDZ, GFP-tagged SNX27, and Flag-tagged SNX27 full-length and the SNX27ΔPDZ and ΔFERM mutants were kindly provided by Martin P. Playford and have been described previously (8, 48, 49).

Mass spectrometry analysis

HeLa cells stably expressing GFP-SNX27 were transfected with a control siRNA or siRNA E6AP to reduce levels of HPV-18E6 expression. After 72 h, the cells were extracted in mass spectrometry lysis buffer [50 mM HEPES, pH 7.4, 150 mM NaCl, 50 mM NaF, 1 mM EDTA, 0.25% NP-40] and incubated with GFP Trap (Chromotek) for 2–3 h on a rotating wheel at 4°C. The beads were then extensively washed, and the samples were subjected to mass spectroscopic analysis, as previously described (8, 50). The interacting partners of SNX27 were compared between control and siRNA E6AP-treated cells. Briefly, proteins were eluted directly from the affinity beads using 50 ng of sequencing grade trypsin (Promega) in 20 mM diammonium phosphate pH 8.0 for 6 h at 37°C. The supernatant was removed from the beads, and the cysteines were reduced and alkylated by boiling for 2 min in the presence of 10 mM Tris (2-carboxyethyl) phosphine (Pierce), followed by incubation with 20 mM acetaminophen (Sigma) for 1 h at 37°C. The reactions were stopped by adding acetic acid (Sigma) to 0.1%. The resulting mixture was desalted using C18 Ziptips (Millipore) and lyophilized to dryness. Nanobore columns were constructed using Picofrit columns (NewObjective) packed with 15 cm of 1.8 mm Zorbax XDB C18 particles using a homemade high-pressure column loader. The desalted samples were injected into the nanobore column in buffer A (10% methanol/0.1% formic acid). The column was developed with a discontinuous gradient and sprayed directly into the orifice of an LTQ ion trap mass spectrometer (Thermo Electron). A cycle of one full scan (400–1,700 *m/z*), followed by eight data-dependent MS/MS scans at 25% normalized collision energy, was performed throughout the LC separation. RAW files from the LTQ were converted to mzXML files by rEADW (version 1.6) and searched against the Ensembl human protein database.

GST pull-down assay

GST-tagged fusion proteins were expressed and purified as described previously (8, 36). HEK293 cells were harvested and lysed in HNTG buffer (20 mM HEPES, pH 7.5, 150 mM NaCl, 0.1% Triton X-100, 10% glycerol), containing protease inhibitors (Calbiochem Protease Cocktail 1). The extracts were clarified by centrifugation and then incubated with the SNX27 GST fusion proteins for 2 h at room temperature. After extensive washing, the bound proteins were analyzsed by SDS PAGE and western blotting.

Co-immunoprecipitation assay

HEK293 cells were transfected with plasmids expressing EMILIN2 and Flag-SNX27 in the presence of GFP-18E6, EMILIN2, and Flag-SNX27 alone, and EMILIN2 together with GFP-18E6 as control. Forty-eight hours after transfection, cells were harvested in HNTG buffer described above, containing protease inhibitors (Calbiochem Protease Cocktail 1), and extracts were immunoprecipitated using an anti-Flag antibody and protein G-conjugated sepharose beads. Co-immunoprecipitating EMILIN2 was then detected by Western blotting using a mouse anti-EMILIN2 antibody (MyBioSource). To verify the interaction of EMILIN2 with WNT1 ligand, HEK293 cells were transfected with plasmids expressing EMILIN2, Flag-tagged SNX27, and V5-tagged WNT1 in the presence of GFP-tagged 18E6 wild-type or 18E6ΔPBM mutant. Cells not expressing V5-tagged WNT1 plasmid were used as control. After 48 h, cells were harvested in HNTG buffer containing protease inhibitors (Calbiochem Protease Cocktail 1), and extracts were immunoprecipitated using an anti-Flag antibody and protein G-conjugated sepharose beads. Co-immunoprecipitating EMILIN2 and SNX27 were then detected by Western blotting using a mouse anti-EMILIN2 antibody and a mouse anti-Flag antibody, respectively.

Analysis of secreted EMILIN2

Twenty-four hours after transfection with appropriate plasmids (HEK293) or 48 h after adding siRNA (Hela), cells were washed twice with PBS and grown in serum-free medium

for another 24 h. Next conditioned media from the cell lines were concentrated using Amicon Ultra-4 centrifugal devices. Equal amounts of proteins were mixed with Laemmli Sample Buffer 6× and run on a 10% SDS-PAGE. To detect EMILIN2 in the medium of HeLa cells, equal amounts of concentrated proteins were immunoprecipitated using an anti-EMILIN2 antibody and protein G-conjugated sepharose beads. Immunoprecipitating EMILIN2 was then detected by Western blotting using a mouse anti-EMILIN2 antibody (MyBioSource).

Immunofluorescence assay

HEK293 cells were seeded on glass coverslips at a density of approximately 5×10^5 cells/coverslip and transfected with GFP-18E6 or 18E6ΔPBM in the presence or absence of EMILIN2. After 48 h, cells were fixed with 4% paraformaldehyde and permeabilized with PBS/0.1% Triton X-100. Immunostaining was performed using rabbit EMILIN2 and mouse GFP antibody (Santa Cruz) and the appropriate fluorophore-conjugated secondary antibodies. The images were captured using the LSM510 META Confocal Microscope (Carl Zeiss).

Colony formation assay

HaCaT cells were seeded in 6 cm plates at the low confluence (15,000 cells/dish). After 24 h, cells were transfected with plasmids expressing either HPV-18E6 WT or HPV-18E6ΔPBM, in the presence or absence of EMILIN2-expressing plasmid, and were selected for 14–21 days with G418 (Invitrogen). Colonies were then stained with Giemsa stain (1% crystal violet, 25% methanol) and counted using the software Plot Histograms of Colony Size (countPHICS) (51). Each experiment was repeated a minimum of three times.

Luciferase assay

HEK293 cells were transfected with plasmids expressing β-catenin and TCF-4 and β-galactosidase (reporter plasmid), and additionally with constructs expressing EMILIN2 alone or with HPV-18E6 or HPV-18E6ΔPBM. Forty-eight hours after transfection, cells were lysed, and luciferase activity was analyzed using Dual Luciferase Assay Kit (Promega) and normalized to *Renilla* following measurement with a luminometer.

Statistical analysis

All experiments were performed with appropriate repetitions. Statistical significance was calculated using the GraphPad Prism 6 software.

ACKNOWLEDGMENTS

We are most grateful to Miranda Thomas for her valuable comments on the manuscript. We express our thanks to Maurizio Mongiat and Martin P. Playford for kindly providing plasmids.

This work was supported by a research grant from the Associazione Italiana per la Ricerca sul Cancro (Progetto IG 2019 ID 23572). J.B. gratefully acknowledges support from the Umberto Veronesi Foundation (postdoctoral fellowship, years 2018, 2020, and 2022).

AUTHOR AFFILIATIONS

[1]International Centre for Genetic Engineering and Biotechnology, Trieste, Italy
[2]Department of Molecular Virology, Adam Mickiewicz University, Poznan, Poland

AUTHOR ORCIDs

Justyna Broniarczyk http://orcid.org/0000-0002-8621-0556
Oscar Trejo-Cerro http://orcid.org/0000-0002-3203-6193
Lawrence Banks http://orcid.org/0000-0003-4360-5731

FUNDING

Funder	Grant(s)	Author(s)
Fondazione Italiana per la Ricerca sul Cancro	ID 23572	Lawrence Banks

AUTHOR CONTRIBUTIONS

Justyna Broniarczyk, Conceptualization, Data curation, Formal analysis, Investigation, Methodology, Validation, Writing – original draft | Oscar Trejo-Cerro, Conceptualization, Formal analysis, Investigation, Methodology | Paola Massimi, Investigation, Methodology | Nežka Kavčič, Formal analysis, Visualization | Michael P. Myers, Formal analysis, Methodology | Lawrence Banks, Conceptualization, Funding acquisition, Methodology, Project administration, Resources, Supervision, Writing – review and editing

DATA AVAILABILITY

Data will be made available on request.

REFERENCES

1. zur Hausen H. 2009. Papillomaviruses in the causation of human cancers - a brief historical account. Virology 384:260–265. https://doi.org/10.1016/j.virol.2008.11.046
2. Ganti K, Broniarczyk J, Manoubi W, Massimi P, Mittal S, Pim D, Szalmas A, Thatte J, Thomas M, Tomaić V, Banks L. 2015. The human papillomavirus E6 PDZ binding motif: from life cycle to malignancy. Viruses 7:3530–3551. https://doi.org/10.3390/v7072785
3. Thomas M, Myers MP, Massimi P, Guarnaccia C, Banks L. 2016. Analysis of multiple HPV E6 PDZ interactions defines type-specific PDZ fingerprints that predict oncogenic potential. PLoS Pathog 12:e1005766. https://doi.org/10.1371/journal.ppat.1005766
4. Thomas M, Banks L. 2021. The biology of papillomavirus PDZ associations: what do they offer papillomaviruses? Curr Opin Virol 51:119–126. https://doi.org/10.1016/j.coviro.2021.09.011
5. Banks L, Pim D, Thomas M. 2012. Human tumour viruses and the deregulation of cell polarity in cancer. Nat Rev Cancer 12:877–886. https://doi.org/10.1038/nrc3400
6. Rozenblatt-Rosen O, Deo RC, Padi M, Adelmant G, Calderwood MA, Rolland T, Grace M, Dricot A, Askenazi M, Tavares M, et al. 2012. Interpreting cancer genomes using systematic host network perturbations by tumour virus proteins. Nature 487:491–495. https://doi.org/10.1038/nature11288
7. Ganti K, Massimi P, Manzo-Merino J, Tomaić V, Pim D, Playford MP, Lizano M, Roberts S, Kranjec C, Doorbar J, Banks L. 2016. Interaction of the human papillomavirus E6 oncoprotein with sorting nexin 27 modulates endocytic cargo transport pathways. PLoS Pathog 12:e1005854. https://doi.org/10.1371/journal.ppat.1005854
8. Broniarczyk JK, Massimi P, Trejo-Cerro O, Myers MP, Banks L. 2022. HPV-18E6 inhibits interactions between TANC2 and SNX27 in a PBM-dependent manner and promotes increased cell proliferation. J Virol 96:e0136522. https://doi.org/10.1128/jvi.01365-22
9. Steinberg F, Gallon M, Winfield M, Thomas EC, Bell AJ, Heesom KJ, Tavaré JM, Cullen PJ. 2013. A global analysis of SNX27-retromer assembly and cargo specificity reveals a function in glucose and metal ion transport. Nat Cell Biol 15:461–471. https://doi.org/10.1038/ncb2721
10. Gogl G, Zambo B, Kostmann C, Cousido-Siah A, Morlet B, Durbesson F, Negroni L, Eberling P, Jané P, Nominé Y, Zeke A, Østergaard S, Monsellier É, Vincentelli R, Travé G. 2022. Quantitative fragmentomics allow affinity mapping of interactomes. Nat Commun 13:5472. https://doi.org/10.1038/s41467-022-33018-0
11. Clairfeuille T, Mas C, Chan ASM, Yang Z, Tello-Lafoz M, Chandra M, Widagdo J, Kerr MC, Paul B, Mérida I, Teasdale RD, Pavlos NJ, Anggono V, Collins BM. 2016. A molecular code for endosomal recycling of phosphorylated cargos by the SNX27-retromer complex. Nat Struct Mol Biol 23:921–932. https://doi.org/10.1038/nsmb.3290
12. Chandra M, Kendall AK, Jackson LP. 2021. Toward understanding the molecular role of SNX27/retromer in human health and disease. Front Cell Dev Biol 9:642378. https://doi.org/10.3389/fcell.2021.642378
13. Deb S, Sun J. 2022. Endosomal sorting protein SNX27 and its emerging roles in human cancers. Cancers (Basel) 15:70. https://doi.org/10.3390/cancers15010070
14. Tomaić V, Pim D, Banks L. 2009. The stability of the human papillomavirus E6 oncoprotein is E6AP dependent. Virology 393:7–10. https://doi.org/10.1016/j.virol.2009.07.029
15. Da Ros F, Persano L, Bizzotto D, Michieli M, Braghetta P, Mazzucato M, Bonaldo P. 2022. Emilin-2 is a component of bone marrow extracellular matrix regulating mesenchymal stem cell differentiation and hematopoietic progenitors. Stem Cell Res Ther 13:2. https://doi.org/10.1186/s13287-021-02674-2
16. Dizanzo MP, Marziali F, Brunet Avalos C, Bugnon Valdano M, Leiva S, Cavatorta AL, Gardiol D. 2020. HPV E6 and E7 oncoproteins cooperatively alter the expression of disc large 1 polarity protein in epithelial cells. BMC Cancer 20:293. https://doi.org/10.1186/s12885-020-06778-5
17. Marastoni S, Andreuzzi E, Paulitti A, Colladel R, Pellicani R, Todaro F, Schiavinato A, Bonaldo P, Colombatti A, Mongiat M. 2014. EMILIN2 down-modulates the Wnt signalling pathway and suppresses breast cancer cell growth and migration. J Pathol 232:391–404. https://doi.org/10.1002/path.4316
18. Bello JOM, Nieva LO, Paredes AC, Gonzalez AMF, Zavaleta LR, Lizano M. 2015. Regulation of the Wnt/β-catenin signaling pathway by human papillomavirus E6 and E7 oncoproteins. Viruses 7:4734–4755. https://doi.org/10.3390/v7082842
19. Mongiat M, Ligresti G, Marastoni S, Lorenzon E, Doliana R, Colombatti A. 2007. Regulation of the extrinsic apoptotic pathway by the extracellular matrix glycoprotein EMILIN2. Mol Cell Biol 27:7176–7187. https://doi.org/10.1128/MCB.00696-07
20. Colombatti A, Doliana R, Bot S, Canton A, Mongiat M, Mungiguerra G, Paron-Cilli S, Spessotto P. 2000. The EMILIN protein family. Matrix Biol 19:289–301. https://doi.org/10.1016/s0945-053x(00)00074-3

21. Colombatti A, Spessotto P, Doliana R, Mongiat M, Bressan GM, Esposito G. 2011. The EMILIN/Multimerin family. Front Immunol 2:93. https://doi.org/10.3389/fimmu.2011.00093
22. Popova NV, Jücker M. 2022. The functional role of extracellular matrix proteins in cancer. Cancers (Basel) 14:238. https://doi.org/10.3390/cancers14010238
23. Andreuzzi E, Fejza A, Capuano A, Poletto E, Pivetta E, Doliana R, Pellicani R, Favero A, Maiero S, Fornasarig M, Cannizzaro R, Iozzo RV, Spessotto P, Mongiat M. 2020. Deregulated expression of elastin microfibril interfacer 2 (EMILIN2) in gastric cancer affects tumor growth and angiogenesis. Matrix Biol Plus 6–7:100029. https://doi.org/10.1016/j.mbplus.2020.100029
24. Andreuzzi E, Fejza A, Polano M, Poletto E, Camicia L, Carobolante G, Tarticchio G, Todaro F, Di Carlo E, Scarpa M, Scarpa M, Paulitti A, Capuano A, Canzonieri V, Maiero S, Fornasarig M, Cannizzaro R, Doliana R, Colombatti A, Spessotto P, Mongiat M. 2022. Colorectal cancer development is affected by the ECM molecule EMILIN-2 hinging on macrophage polarization via the TLR-4/MyD88 pathway. J Exp Clin Cancer Res 41:60. https://doi.org/10.1186/s13046-022-02271-y
25. Zhao G, Zheng J, Tang K, Chen Q. 2022. EMILIN2 is associated with prognosis and immunotherapy in clear cell renal cell carcinoma. Front Genet 13:1058207. https://doi.org/10.3389/fgene.2022.1058207
26. Tang X, Li F. 2022. Decreased EMILIN2 correlates to metabolism phenotype and poor prognosis of ovarian cancer. J Biochem 172:89–97. https://doi.org/10.1093/jb/mvac046
27. Joubert L, Hanson B, Barthet G, Sebben M, Claeysen S, Hong W, Marin P, Dumuis A, Bockaert J. 2004. New sorting nexin (SNX27) and NHERF specifically interact with the 5-HT4a receptor splice variant: roles in receptor targeting. J Cell Sci 117:5367–5379. https://doi.org/10.1242/jcs.01379
28. Lunn M-L, Nassirpour R, Arrabit C, Tan J, McLeod I, Arias CM, Sawchenko PE, Yates III JR, Slesinger PA. 2007. A unique sorting nexin regulates trafficking of potassium channels via a PDZ domain interaction. Nat Neurosci 10:1249–1259. https://doi.org/10.1038/nn1953
29. MacNeil AJ, Mansour M, Pohajdak B. 2007. Sorting nexin 27 interacts with the Cytohesin associated scaffolding protein (CASP) in lymphocytes. Biochem Biophys Res Commun 359:848–853. https://doi.org/10.1016/j.bbrc.2007.05.162
30. Rincón E, Sáez de Guinoa J, Gharbi SI, Sorzano COS, Carrasco YR, Mérida I. 2011. Translocation dynamics of sorting nexin 27 in activated T cells. J Cell Sci 124:776–788. https://doi.org/10.1242/jcs.072447
31. Lauffer BEL, Melero C, Temkin P, Lei C, Hong W, Kortemme T, von Zastrow M. 2010. SNX27 mediates PDZ-directed sorting from endosomes to the plasma membrane. J Cell Biol 190:565–574. https://doi.org/10.1083/jcb.201004060
32. Ghai R, Collins BM. 2011. PX-FERM proteins: a link between endosomal trafficking and signaling? Small GTPases 2:259–263. https://doi.org/10.4161/sgtp.2.5.17276
33. Ghai R, Mobli M, Norwood SJ, Bugarcic A, Teasdale RD, King GF, Collins BM. 2011. Phox homology band 4.1/ezrin/radixin/moesin-like proteins function as molecular scaffolds that interact with cargo receptors and Ras GTPases. Proc Natl Acad Sci U S A 108:7763–7768. https://doi.org/10.1073/pnas.1017110108
34. Sharma P, Parveen S, Shah LV, Mukherjee M, Kalaidzidis Y, Kozielski AJ, Rosato R, Chang JC, Datta S. 2020. SNX27-retromer assembly recycles MT1-MMP to invadopodia and promotes breast cancer metastasis. J Cell Biol 219:e201812098. https://doi.org/10.1083/jcb.201812098
35. Nourry C, Grant SGN, Borg J-P. 2003. PDZ domain proteins: plug and play!Sci STKE 2003:RE7. https://doi.org/10.1126/stke.2003.179.re7
36. Paulitti A, Andreuzzi E, Bizzotto D, Pellicani R, Tarticchio G, Marastoni S, Pastrello C, Jurisica I, Ligresti G, Bucciotti F, Doliana R, Colladel R, Braghetta P, Poletto E, Di Silvestre A, Bressan G, Colombatti A, Bonaldo P, Mongiat M. 2018. The ablation of the matricellular protein EMILIN2 causes defective vascularization due to impaired EGFR-dependent IL-8 production affecting tumor growth. Oncogene 37:3399–3414. https://doi.org/10.1038/s41388-017-0107-x
37. Sun L, Hu X, Chen W, He W, Zhang Z, Wang T. 2016. Sorting nexin 27 interacts with Fzd7 and mediates Wnt signalling. Biosci Rep 36:e00296. https://doi.org/10.1042/BSR20150205
38. DuChez BJ, Hueschen CL, Zimmerman SP, Baumer Y, Wincovitch S, Playford MP. 2019. Characterization of the interaction between β-catenin and sorting nexin 27: contribution of the type I PDZ-binding motif to Wnt signaling. Biosci Rep 39:BSR20191692. https://doi.org/10.1042/BSR20191692
39. Lichtig H, Gilboa DA, Jackman A, Gonen P, Levav-Cohen Y, Haupt Y, Sherman L. 2010. HPV16 E6 augments Wnt signaling in an E6AP-dependent manner. Virology 396:47–58. https://doi.org/10.1016/j.virol.2009.10.011
40. Yang Z, Liu H, Song R, Lu W, Wang H, Gu S, Cao X, Chen Y, Liang J, Qin Q, Yang X, Feng D, He J. 2021. Reduced MAGI3 level by HPV18E6 contributes to Wnt/β-catenin signaling activation and cervical cancer progression. FEBS Open Bio 11:3051–3062. https://doi.org/10.1002/2211-5463.13298
41. Muñoz-Bello JO, Olmedo-Nieva L, Castro-Muñoz LJ, Manzo-Merino J, Contreras-Paredes A, González-Espinosa C, López-Saavedra A, Lizano M. 2018. HPV-18 E6 oncoprotein and its spliced isoform E6*I regulate the Wnt/β-Catenin cell signaling pathway through the TCF-4 transcriptional factor. Int J Mol Sci 19:3153. https://doi.org/10.3390/ijms19103153
42. Herbster S, Paladino A, de Freitas S, Boccardo E. 2018. Alterations in the expression and activity of extracellular matrix components in HPV-associated infections and diseases. Clinics (Sao Paulo) 73:e551s. https://doi.org/10.6061/clinics/2018/e551s
43. Joana S, Joana F, Ana Carolina S, Manuel B, Maria Clara B. 2021. The importance of the extracellular matrix in HPV-associated diseases. In Rajamanickam R (ed), Cervical cancer. IntechOpen, Rijeka.
44. Allen-Hoffmann BL, Schlosser SJ, Ivarie CA, Sattler CA, Meisner LF, O'Connor SL. 2000. Normal growth and differentiation in a spontaneously immortalized near-diploid human keratinocyte cell line, NIKS. J Invest Dermatol 114:444–455. https://doi.org/10.1046/j.1523-1747.2000.00869.x
45. Graham FL, van der Eb AJ. 1973. A new technique for the assay of infectivity of human adenovirus 5 DNA. Virology 52:456–467. https://doi.org/10.1016/0042-6822(73)90341-3
46. Pim D, Thomas M, Javier R, Gardiol D, Banks L. 2000. HPV E6 targeted degradation of the discs large protein: evidence for the involvement of a novel ubiquitin ligase. Oncogene 19:719–725. https://doi.org/10.1038/sj.onc.1203374
47. Thatte J, Massimi P, Thomas M, Boon SS, Banks L. 2018. The human papillomavirus E6 PDZ binding motif links DNA damage response signaling to E6 inhibition of P53 transcriptional activity. J Virol 92:e00465-18. https://doi.org/10.1128/JVI.00465-18
48. Valdes JL, Tang J, McDermott MI, Kuo JC, Zimmerman SP, Wincovitch SM, Waterman CM, Milgram SL, Playford MP. 2011. Sorting nexin 27 protein regulates trafficking of a P21-activated kinase (PAK) interacting exchange factor (β-Pix)-G protein-coupled receptor kinase interacting protein (GIT) complex via a PDZ domain interaction. J Biol Chem 286:39403–39416. https://doi.org/10.1074/jbc.M111.260802
49. Pim D, Broniarczyk J, Bergant M, Playford MP, Banks L. 2015. A novel PDZ domain interaction mediates the binding between human papillomavirus 16 L2 and sorting nexin 27 and modulates virion trafficking. J Virol 89:10145–10155. https://doi.org/10.1128/JVI.01499-15
50. Tomaić V, Gardiol D, Massimi P, Ozbun M, Myers M, Banks L. 2009. Human and primate tumour viruses use PDZ binding as an evolutionarily conserved mechanism of targeting cell polarity regulators. Oncogene 28:1–8. https://doi.org/10.1038/onc.2008.365
51. Brzozowska B, Gałecki M, Tartas A, Ginter J, Kaźmierczak U, Lundholm L. 2019. Freeware tool for analysing numbers and sizes of cell colonies. Radiat Environ Biophys 58:109–117. https://doi.org/10.1007/s00411-018-00772-z